Virology 387 (2009) 353–363

Contents lists available at ScienceDirect

Virology

journal homepage: www.elsevier.com/locate/yviro

Polycistronic mRNAs and internal ribosome entry site elements (IRES) are widely used by white spot syndrome virus (WSSV) structural protein genes

Shih-Ting Kang [a], Jiann-Horng Leu [a,c], Han-Ching Wang [b], Li-Li Chen [d], Guang-Hsiung Kou [a,*], Chu-Fang Lo [a,*]

[a] Institute of Zoology, National Taiwan University, Taipei 106, Taiwan
[b] Institute of Biotechnology, National Cheng Kung University, Tainan, Taiwan
[c] Center for marine bioscience and biotechnology, National Taiwan Ocean university, Keelung, Taiwan
[d] Institute of Marine Biology, National Taiwan Ocean University, Keelung, Taiwan

ARTICLE INFO

Article history:
Received 27 November 2008
Returned to author for revision
6 January 2009
Accepted 6 February 2009
Available online 14 March 2009

Keywords:
Polycistronic mRNA
IRES
WSSV
Gene cluster
Penaeus monodon

ABSTRACT

The genome of the white spot syndrome virus (WSSV) Taiwan isolate has many structural and non-structural genes that are arranged in clusters. Screening with Northern blots showed that at least four of these clusters produce polycistronic mRNA, and one of these (*vp31*/*vp39b*/*vp11*) was studied in detail. The *vp31*/*vp39b*/*vp11* cluster produces two transcripts, including a large 3.4-kb polycistronic transcript of all three genes. No monocistronic *vp39b* mRNA was detected. TNT and *in vitro* translation assays showed that *vp39b* translation was independent of *vp31* translation, and that ribosomal reinitiation was not a possible mechanism for *vp39b*. An unusually located IRES (internal ribosome entry site) element was identified in the *vp31*/*vp39b* coding region, and this region was able to promote the expression of a downstream firefly luciferase reporter. We show that *vp31*/*vp39b*/*vp11* is representative of many other WSSV structural/non-structural gene clusters, and argue that these are also likely to produce polycistronic mRNAs and that use an IRES mechanism to regulate their translation.

Introduction

While the eukaryotes can use either cap-dependent or cap-independent translation mechanisms, most cellular mRNAs utilize the cap-dependent mechanism for protein translation. In this mechanism, translation initiation factors recognize the 5′ cap structure (m^7GpppN) first, and then the 43S pre-initiation complex is recruited (Kozak, 1978; Pestova et al., 1998). Next, the 43S pre-initiation complex scans along the mRNA to locate the first favorable initiation codon (usually ATG), with which it forms a 48S complex. The subsequent addition of a 60S ribosomal subunit leads to the formation of an 80S initiation complex, and this begins the translation. Cap-independent translation was first discovered at an internal ribosome entry site (IRES) of poliovirus, where an RNA secondary structure in the 5′ untranslated region (5′ UTR) mediated internal translation without a 5′ cap structure (Pelletier and Sonenberg, 1988). Many IRES elements have since been identified in other positive-sense RNA viruses, such as hepatitis C virus (Tsukiyama-Kohara et al., 1992) and encephalomyocarditis virus (Jang et al., 1988), as well as in cellular mRNAs that are involved in the cell cycle or cell survival (http://www.rangueil.inserm.fr/iresdatabase). In the DNA viruses, the first IRES was discovered in Kaposi's sarcoma-associated Herpesvirus (KSHV), where a novel IRES element is located in the coding region of vCyclin (Bieleski and Talbot, 2001; Grundhoff and Ganem, 2001; Low et al., 2001). Since then, only a few IRESs have been identified in DNA viral genomes. These include the IRES in the thymidine kinase gene of herpes simplex virus (HSV; Griffiths and Coen, 2005), the IRES upstream of the *vp3* coding region of simian virus 40 (SV40; Yu and Alwine, 2006), and the IRES upstream of *vp28* in the shrimp pathogen WSSV (Han and Zhang, 2006).

WSSV is an enveloped, ellipsoid, large double-stranded DNA virus (Wang et al., 1995) with a genome of about 300 kbp. WSSV isolates from China (WSSV-CN, GenBank accession no. AF332093; Yang et al., 2001), Taiwan (WSSV-TW, GenBank accession no. AF440570; Wang et al., 1995), and Thailand (WSSV-TH, GenBank accession no. AF369029; van Hulten et al., 2001) have been completely sequenced. The WSSV-TW genome encodes 532 predicted open reading frames (ORFs) that consist of more than 60 amino acids. About 30% of these ORFs have a polyadenylation signal (AATAAA) within the ORF or downstream of their stop codon. For the WSSV structural proteins, the proportion of genes with a poly(A) signal rises to over 60% (24 of 39), while the remainder (15 of 39) have no such signal (Tsai et al., 2004). The structural protein genes with the poly(A) signal are distributed fairly evenly around the circular WSSV genome; conversely, the structural genes lacking a poly(A) signal are always located in clusters, some of which also include non-structural genes (Tsai et al., 2004). The intergenic regions in these clusters are usually small, and genes in the same cluster tend to have the same transcriptional orientation.

* Corresponding authors. Fax: +886 2 23638179.
E-mail addresses: ghkou@ntu.edu.tw (G.-H. Kou), gracelow@ntu.edu.tw (C.-F. Lo).

0042-6822/$ – see front matter © 2009 Elsevier Inc. All rights reserved.
doi:10.1016/j.virol.2009.02.012

Furthermore, in some gene clusters such as *vp31/vp39b/vp11*, *vp22/vp39a/wssv363/vp51c*, and *vp60b/wssv478/wssv479/vp28*, the polyadenylation signal is only found within the ORF or in the 3′ UTR of the last gene, while the preceding genes have no poly(A) signal within their ORF or 3′ UTR. This suggests that these clustered genes may share a long transcript with the same poly(A) tail (Tsai et al., 2004).

Previous studies have found that polycistronic mRNAs were transcribed from clusters of WSSV genes. For example: two transcripts, a polycistronic mRNA of about 5.5 kb and a monocistronic mRNA of about 1.3 kb, were detected using a *vp35*-specific riboprobe (Chen et al., 2002); two transcripts, a polycistronic mRNA of about 4.5 kb and a monocistronic mRNA of about 1.4 kb, were detected from the *wssv237/wssv240/wssv243* cluster using a *rr2*-specific riboprobe (*wssv243* encodes Ribonucleotide Reductase 2, RR2; Tsai et al., 2000); and two transcripts, a polycistronic mRNA of about 5.7 kb and a monocistronic mRNA of about 2.7 kb, were detected using a *protein kinase 1*-specific riboprobe (Liu et al., 2001). In addition, an IRES element in the 5′ UTR of *vp28* was discovered by Han and Zhang (2006). In the present study, we used Northern blot analyses to show that polycistronic mRNA was being transcribed from the *vp60b/wssv478/wssv479/vp28* cluster and from three other clusters, *vp31/vp39b/vp11*, *wssv130/wssv133/vp36a*, and *vp36b/vp51b/vp38a*. To further investigate the gene expression mechanism of one of these gene clusters, *vp31/vp39b/vp11*, we first used 5′/3′ RACE and found that two transcripts produced by this gene cluster were a 3.4-kb *vp31/vp39b/vp11* polycistronic transcript and a 1.6-kb monocistronic *vp11* transcript. Next we used coupled *in vitro* transcription-translation (TNT) assays, *in vitro* translation assays and dual luciferase activity assays to demonstrate that the expression of *vp39b* from the 3.4 kb transcript is regulated by an IRES element located in the coding region of *vp31/vp39b*. Our results suggest that IRES elements are involved in the expression of WSSV structural genes, and further, that polycistronic mRNAs are widely used to regulate the transcriptional mechanism of other clusters of WSSV structural and non-structural genes.

Results

Polycistronic mRNAs are transcribed by WSSV gene clusters

Fig. 1 shows that polycistronic transcripts were produced by all four of the WSSV gene clusters investigated in this study. Using the

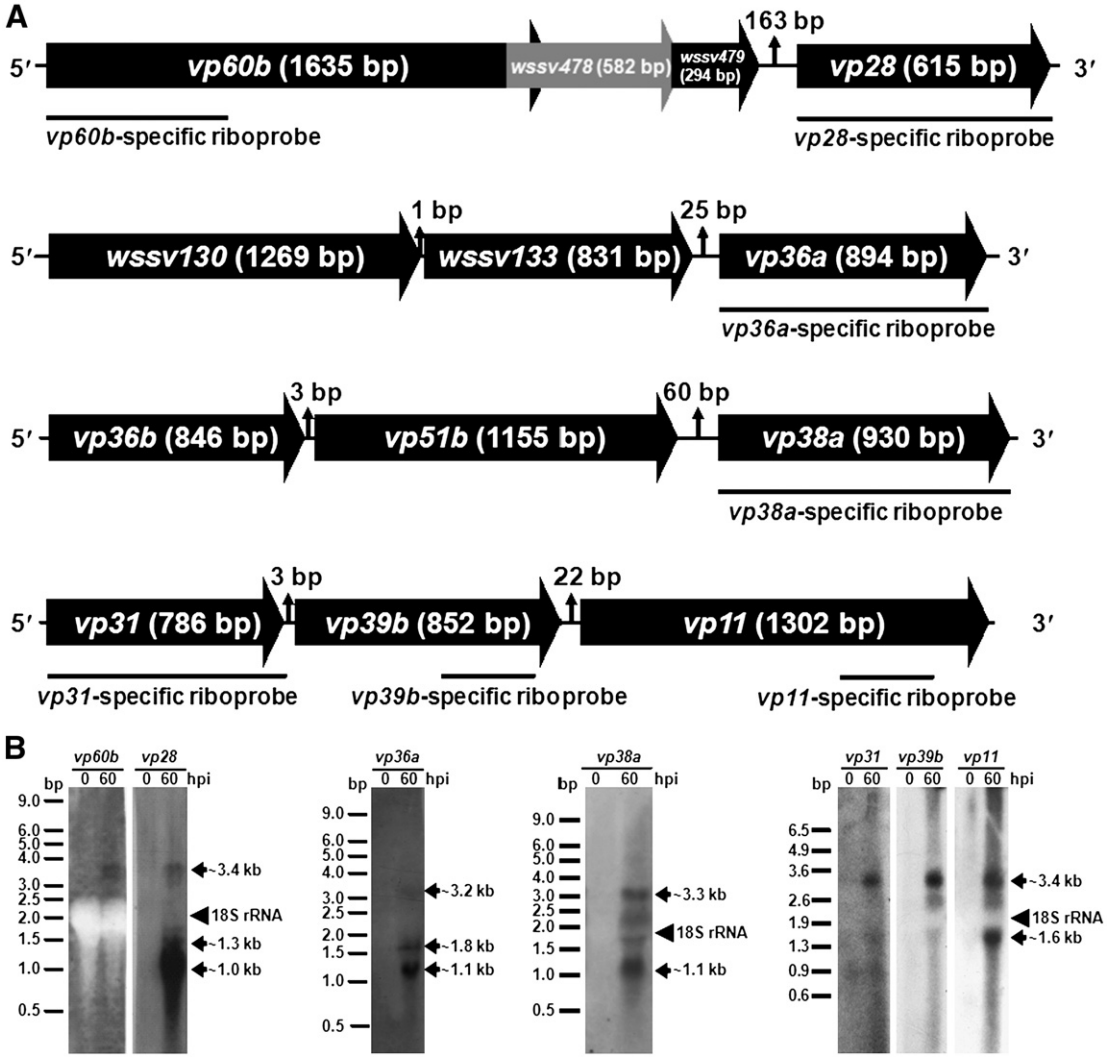

Fig. 1. Polycistronic mRNAs were transcribed from WSSV gene clusters. (A) Schematic diagrams of the WSSV gene clusters *vp60b/wssv478/wssv479/vp28*, *wssv130/wssv133/vp36a*, *vp36b/vp51b/vp38a* and *vp31/vp39b/vp11*. The gene-specific riboprobes used for Northern blot analysis are indicated by solid lines. (B) Northern blot analysis of total RNA isolated from the pleopods or gills of healthy (0 hpi) and WSSV-infected *P. monodon* (60 hpi) using *vp60b*, *vp28*, *vp36a*, *vp38a*, *vp31*, *vp39b* and *vp11*-specific riboprobes. For the first 3 clusters, about 20 μg of total RNA was isolated at 0 and 60 hpi, electrophoresed in the presence of formaldehyde, transferred onto Hybond N^+ nylon membrane and probed with the DIG-labeled gene-specific probes. For the *vp31/vp39b/vp11* cluster, about 30 μg of total RNA was isolated at 0 and 60 hpi, electrophoresed in the presence of formaldehyde, transferred onto Hybond N^+ nylon membrane and probed with the ^{32}P-labeled gene-specific probes. The size standards are based on RNA markers (Amersham Pharmacia Biotech, USA or Promega). The arrows indicate the monocistronic, bicistronic, and polycistronic mRNA transcripts. The 18S rRNA is also indicated (arrowhead).

specific riboprobes (Fig. 1A), Northern blot analyses (Fig. 1B) showed that the *vp60b*/*wssv478*/*wssv479*/*vp28* cluster transcribed: a ~3.4 kb polycistronic mRNA that encoded the *vp60b* and *vp28* proteins (as verified by 5′/3′ RACE analyses; data not shown); a ~1.3 kb bicistronic mRNA that included *wssv479* and *vp28*; and a ~1.0 kb monocistronic mRNA containing only *vp28*. From the *wssv130*/*wssv133*/*vp36a* cluster, three mRNA transcripts were detected: a ~3.2 kb polycistronic mRNA containing all three ORFs; a ~1.8 kb bicistronic mRNA containing *wssv133* and *vp36a*; and a ~1.1 kb monocistronic mRNA containing only the *vp36a* gene. The *vp36b*/*vp51b*/*vp38a* gene cluster transcribed a ~3.3 kb polycistronic mRNA containing all three genes and a ~1.1 kb monocistronic mRNA containing only *vp38a*.

When transcripts from the *vp31*/*vp39b*/*vp11* cluster were detected with the *vp31*-, *vp39b*-, and *vp11*-specific riboprobes, all three probes detected a 3.4-kb band, while the *vp11* probe also hybridized another band of 1.6 kb (Fig. 1B). These results suggest that *vp39b* is only being transcribed as a polycistronic mRNA, in which case the VP39B protein would have to be translated by a cap-independent mechanism. This made the *vp31*/*vp39b*/*vp11* cluster a good subject for further investigation. As a first step, we next used 5′ and 3′ RACE to determine the transcriptional units of *vp31*, *vp39b* and *vp11*.

The wssv396/wssv395/wssv394 gene cluster produces a vp31/vp39b/vp11 polycistronic transcript and a vp11 monocistronic transcript

The sequencing results showed that both *vp31* and *vp39b* had the same two transcription initiation sites (TIS), and that these were located 32 and 35 nt upstream of the translational start codon of *vp31* (**G**TT**G** [the bold and underlined nucleotides are the initiation sites; Fig. 2B]). *vp11* had only one TIS located 205 nucleotides upstream of its translational start codon (T**A**GT; Fig. 2B). The results of 3′ RACE showed that all three genes had the same poly(A) addition site, which was 17 nt downstream of the *vp11* polyadenylation signal (Fig. 2B).

Based on these results, we concluded that this gene cluster transcribes two mRNAs with different 5′ ends but with the same 3′ ends. One transcript is a large, 3.4-kb mRNA encoding all three proteins and the other is a small, 1.6-kb mRNA encoding only VP11.

VP31, VP39B and VP11 are envelope proteins

Our previous proteomic study of purified WSSV virions (Tsai et al., 2004) suggested that the genes of VP31, VP39B and VP11 are viral structural proteins. To confirm this, the respective recombinant proteins were successfully expressed in *E. coli*, the corresponding antibodies were obtained, and Western blotting was used to detect the proteins in the envelope and nucleocapsid viral fractions. All three proteins were located in the envelope fraction (Fig. 3).

The Western blots also revealed the apparent molecular masses of the proteins. The apparent molecular masses of VP31 and VP39B (31 and 39 kDa, respectively) were in good agreement with their calculated molecular masses and also matched well with the previous proteomic results (Tsai et al., 2004). However, while the predicted molecular mass of VP11 is 48 kDa, the gene product of *wssv394* was identified as an 11 kDa protein in the proteomic study (Tsai et al., 2004), and VP11 was detected here as a 38 kDa protein (Fig. 3). One possible explanation for these discrepancies is that *wssv394* does in fact encode a 48 kDa protein, which, after synthesis, is then processed or degraded to the 38 and 11 kDa proteins. In support of this, several candidate proteolytic cleavage sites were predicted using Peptidecutter and other programs (data

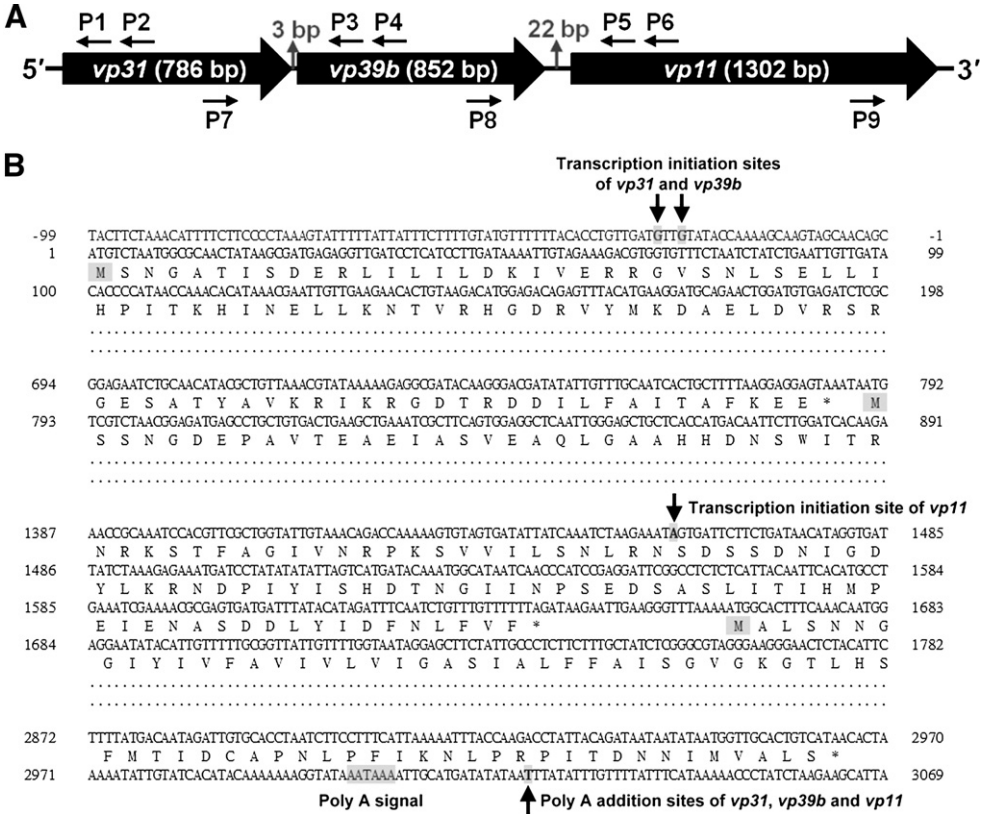

Fig. 2. Mapping the 5′ and 3′ end of the *vp31*, *vp39b* and *vp11* transcripts by 5′/3′ RACE. (A) Schematic diagram showing the locations of the primers used in the 5′/3′ RACE. (P1: *vp31*-5′-RACE-sp2, P2: *vp31*-5′-RACE-sp1, P3: *vp39b*-5′-RACE-sp2, P4: *vp39b*-5′-RACE-sp1, P5: *vp11*-5′-RACE-sp2, P6: *vp11*-5′-RACE-sp1, P7: *wssv397*-R1, P8: *vp39b*-R2, P9: *vp11*-3′RACE; see Table 1.) (B) The deduced amino sequence and corresponding nucleotides of the three genes (*vp31*: nt 1→786; *vp39b*: nt 789→1641; *vp11*: nt 1664→2965). The shaded "M" and asterisk respectively represent the first amino acid methionine and stop codon of each gene. The poly-adenylation signal (AATAAA) is shaded. The transcriptional start sites and the poly "A" addition site are indicated by arrows.

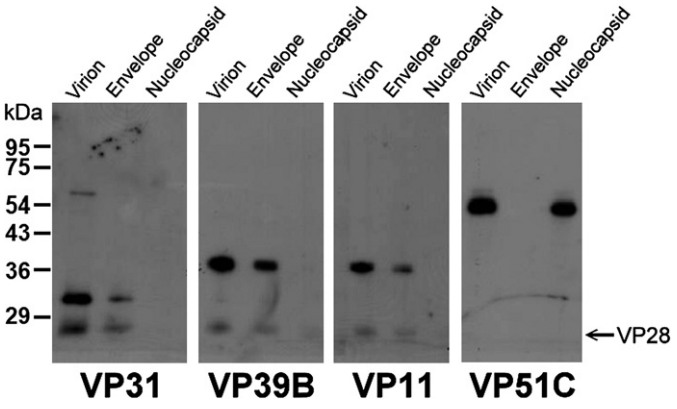

Fig. 3. Western blot analyses of VP31 VP39B and VP11. VP31, VP39B and VP11 were all detected in the purified total WSSV virions and in the envelope fraction. The nucleocapsid protein VP51C (Tsai et al., 2004) was used as a fractionation quality control and was detected only in the total virions and the nucleocapsid fraction. Non-specific signals from the major envelope protein VP28 were also detected by the VP31, VP39B and VP11 antibodies.

not shown). However, if this explanation is correct, then the 48 kDa protein must be very unstable, since it was never detected in the virions by Western blot. However, further study will be needed to test this hypothesis.

vp39b may be translated through an IRES-mediated mechanism

Theoretically, while VP31 and VP11 could both be translated from the corresponding 3.4- and 1.6-kb mRNAs using a cap-dependent mechanism, VP39B can only be translated from the 3.4 kb mRNA through a cap-independent mechanism. It is also possible that *vp11* could be translated from the polycistronic 3.4 kb mRNA, but that possibility was not investigated here. To experimentally confirm that VP39B is being expressed via a cap-independent translational mechanism, a bicistronic expression construct pcDNA3-HA-*vp31*/*vp39b* (Fig. 4A) was assayed by coupled *in vitro* transcription-translation assay. As shown in Fig. 4B, lane 1, this bicistronic construct expressed both proteins, and the signal intensity of VP31 was stronger than that of VP39B. This result confirmed that the translation of VP39B was cap-independent, and since the assay was performed in rabbit reticulocyte lysate (RRL), it

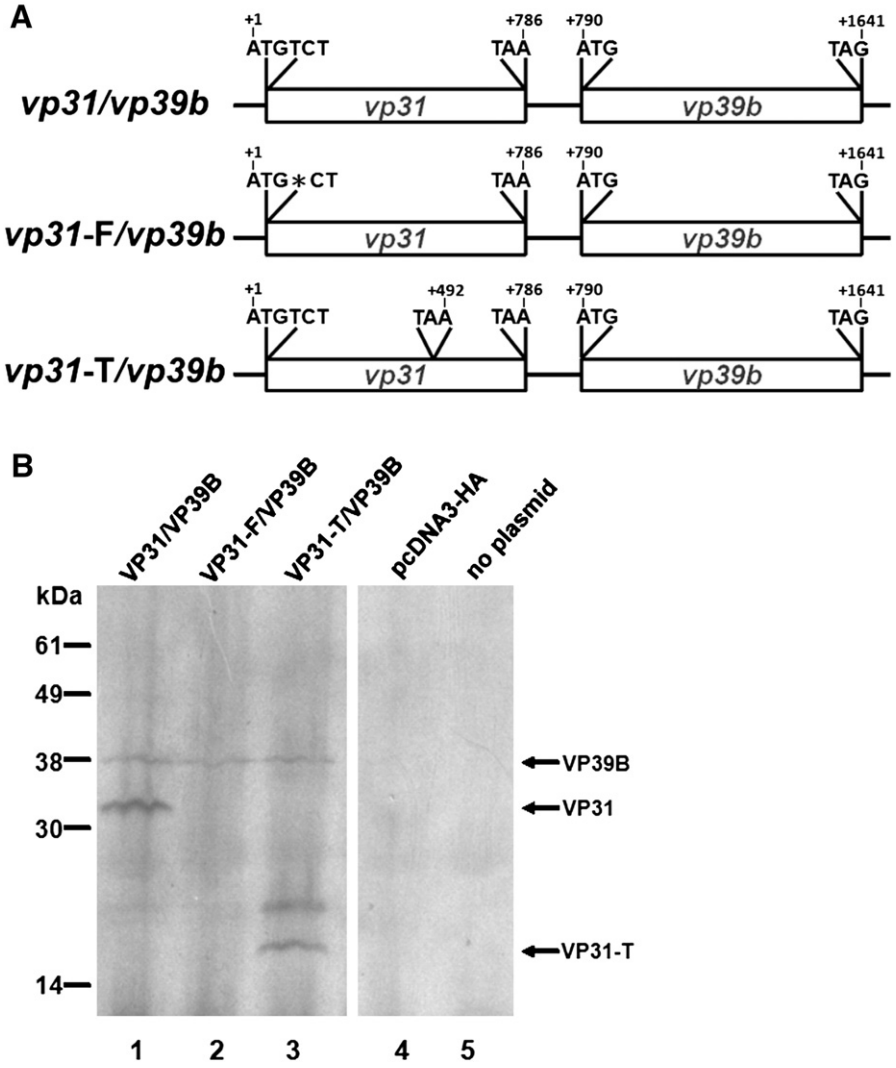

Fig. 4. Coupled *in vitro* transcription-translation of frame-shifted and truncated *vp31*/*vp39b* constructs. (A) Two mutant forms of the pcDNA3-HA-*vp31*/*vp39b* bicistronic plasmid were constructed. In the frame shift mutant, *vp31*-F/*vp39b*, a base from the second codon of *vp31* was deleted to generate a 20-codon nonsense open reading frame. In the truncation mutant, *vp31*-T/*vp39b*, codon 164 of *vp31* was mutated to a stop. (B) Translation products from the indicated constructs. Size standards were determined by protein prestained marker (Bioman).

also showed that the translation required no other viral or shrimp host proteins.

To further explore the cap-independent translational mechanism of *vp39b*, we next tested whether the expression of *vp39b* depends on the expression of *vp31*. To this end, the *vp31*-F/*vp39b* frame shift mutation construct (Fig. 4A) was subjected to the TNT assay. Our results showed that this frame-shifted construct still expressed VP39B (Fig. 4B, lane 2), from which we concluded that the expression of *vp39b* did not require the expression of *vp31*.

Our next assay was to determine which of the two kinds of cap-independent translational mechanism was being used in the expression of VP39B. One mechanism is translational reinitiation, which usually requires an optimal intergenic region of no more than 80 bp and is usually associated with a short upstream ORF (up to 30 codons) (Kozak, 1987). Although the *vp31* gene has 262 codons, there are other known instances of large upstream viral genes that use translational reinitiation to regulate the expression of a downstream ORF (e.g., translational reinitiation is used to transcribe the gene immediately downstream of the feline calicivirus ORF2 gene, which encodes a ~75 kDa precursor of the VP1 protein; Poyry et al., 2007). Therefore, to test if *vp39b* translation occurs through reinitiation, codon 164 of *vp31* was mutated to become a stop codon in the *vp31*-T/*vp39b* construct (Fig. 4A). This mutation not only expressed a truncated VP31 protein but also increased the intergenic distance between *vp31* and *vp39b* from 3 bp to 297 bp. In the TNT assay this construct successfully expressed the VP39b protein (Fig. 4B, lane 3).

In both the *vp31*-F/*vp39b* and *vp31*-T/*vp39b* constructs, the intergenic distance between the mutated *vp31* and *vp39b* was far greater than 80 bp. With such a large intergenic region, we infer that the translation of *vp39b* could not have occurred through translational reinitiation. From the data presented here, we therefore conclude that the expression of *vp39b* must be effected by IRES-mediated internal translation.

The vp31/vp39b coding region is able to regulate firefly luciferase translation in vitro

To further substantiate whether there is a functional IRES element within the *vp31/vp39b* sequence, a partial fragment (nt 123 to 919) of the *vp31/vp39b* coding region (Fig. 5A) was cloned into the upstream region of the firefly luciferase gene in the T7/pRL-

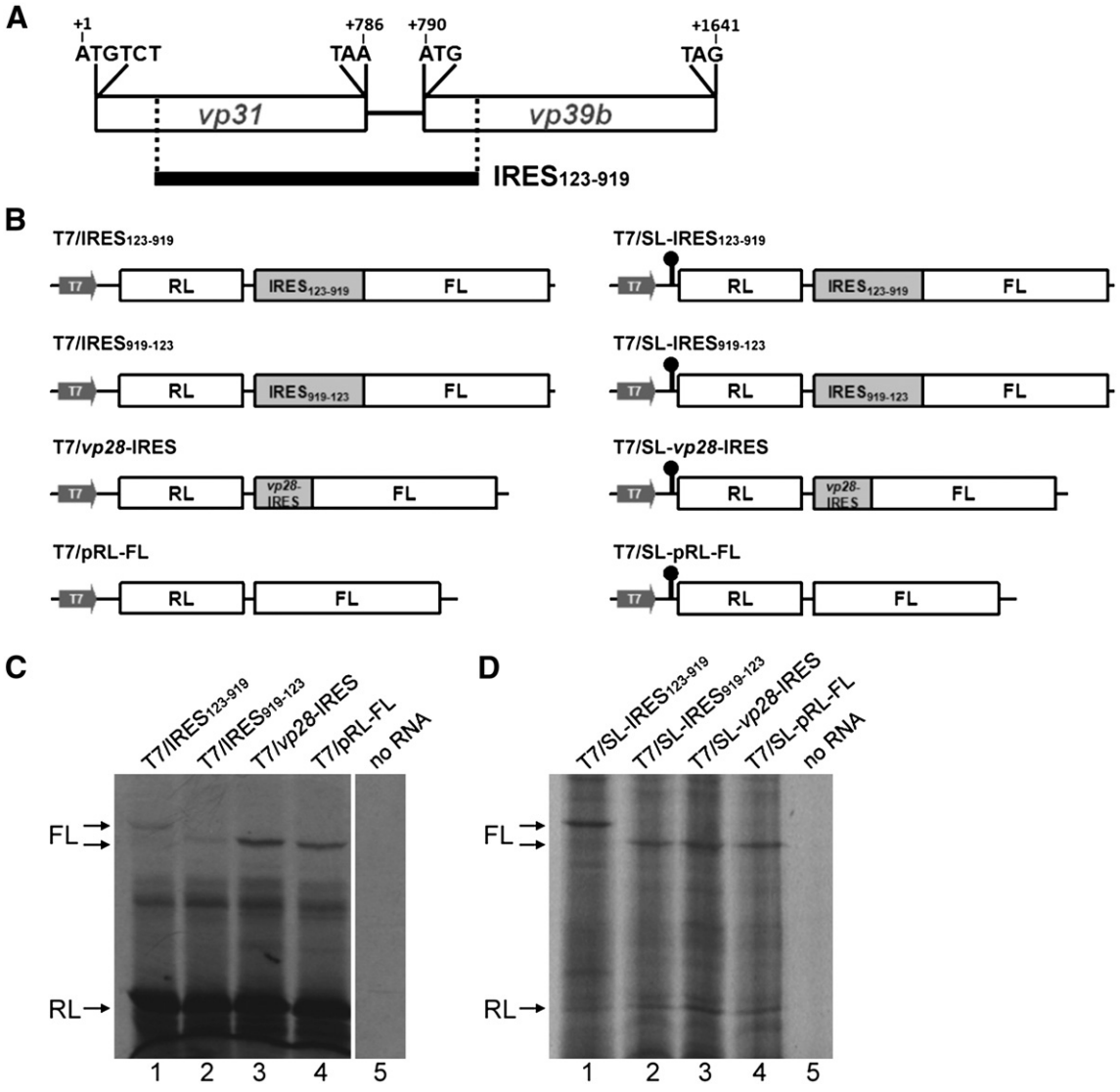

Fig. 5. The *vp31/vp39b* coding region exhibits IRES activity *in vitro*. (A) Location of the putative IRES element in the *vp31/vp39b* coding region. (B) Schematic diagrams of the dicistronic constructs of T7/pRL-FL and T7/SL-pRL-FL (SL: stem–loop). The stable stem–loop structure with a free energy of −62 kcal/mol was introduced upstream of the *Renilla* ORF in the vector T7/SL-pRL-FL. (C) (D) After *in vitro* synthesis with T7 RNA polymerase, the indicated uncapped dicistronic transcripts were translated in Flexi RRL (Promega).

FL plasmid such that the ATG start codon of *vp39b* was fused in-frame with the downstream firefly luciferase. The resultant plasmid was designated T7/IRES$_{123–919}$ (Fig. 5B). As a negative control, the same partial fragment of the *vp31*/*vp39b* coding region was inserted in reverse orientation to generate T7/IRES$_{919–123}$. We also constructed a positive control plasmid T7/*vp28*-IRES that contained the recently identified IRES element from the WSSV *vp28* gene (Han and Zhang, 2006). The dicistronic transcripts produced by these constructs were then translated *in vitro*. Fig. 5C shows that the IRES activity of IRES$_{123–919}$ (lane 1) was weaker than that of the empty vector (lane 4), and it was only slightly higher than the IRES activity of the negative control (IRES$_{919–123}$; lane 2).

However, when a thermodynamically stable stem–loop (SL) was inserted upstream of the RL ORF to block 5′ ribosomal scanning, we found that whereas the upstream RL translation was substantially reduced for all four dicistronic transcripts (cf Figs. 5C and D), the downstream FL translation of the T7/SL-IRES$_{123–919}$ dicistronic transcript was now much greater than that of the other dicistronic transcripts (Fig. 5D). Because the stem–loop blocked ribosomal scanning and greatly reduced the possibility of translational reinitiation, we conclude that the increased expression of FL from the bicistronic transcript of T7/IRES$_{123–919}$ must have been regulated by an IRES element. That is, in this assay, FL translation from the T7/SL-IRES$_{123–919}$ dicistronic transcript occurred independently of RL translation and it was IRES-dependent.

The IRES element is functional in Sf9 cells

To test whether the IRES$_{123–919}$ fragment was functional in Sf9 cells, it was inserted into the upstream region of the firefly luciferase gene in a dual-luciferase reporter plasmid driven by the WSSV *ie1* promoter (Fig. 6). This reporter construct was transfected into Sf9 cells, and 48 h later, the transfected cells were harvested and assayed for *Renilla* luciferase and firefly luciferase activities. The ratio of firefly luciferase activity to *Renilla* luciferase activity was used to represent the IRES activity.

As shown in Fig. 6, the relative luciferase activity of the *ie1*/IRES$_{123–919}$ construct was ~1.7 times higher than that of the positive control (*ie1*/*vp28*-IRES) and ~43 times higher than that of the empty plasmid (*ie1*/pRL-FL). The plasmid with the reversed *vp31*/*vp39b* fragment, *ie1*/IRES$_{919–123}$, showed only a low level of activity. These results indicated that an IRES element was indeed located within the *vp31*/*vp39b* region and its IRES function was directionally dependent.

The transcript from the ie1/IRES$_{123–919}$ bicistronic plasmid does not undergo splicing

It is possible that the firefly luciferase activity from the *ie1*/IRES$_{123–919}$ bicistronic plasmid was due to splicing events that generated an abnormal monocistronic FL transcript. To exclude this possibility, total RNAs were isolated from *ie1*/IRES$_{123–919}$-transfected (T) or untransfected (UT) Sf9 cells and subjected to RT-PCR analysis with two primer sets that amplified overlapping fragments of the entire transcript (Fig. 7A). The results (Fig. 7B) showed that only one RT-PCR product was amplified by each primer set (P1/P2 lane 2; P3/P4 lane 2), and in both cases, the product had the expected size as verified by the plasmid DNA templates (lane 4). Sequence analysis of these two bands also showed the presence of full-length bicistronic RNA and no smaller RNA species. We therefore conclude that when the *ie1*/IRES$_{123–919}$ bicistronic plasmid is transfected into Sf9 cells, no RNA splicing events occur.

Discussion

The evidence presented here shows that the structural protein gene cluster *vp31*/*vp39b*/*vp11* transcribes a 3.4 kb polycistronic mRNA and uses an IRES element to regulate the expression of *vp39b*. Northern blot and 5′/3′ RACE analyses of tissues from WSSV-infected shrimp (Figs. 1 and 2) detected only a single species of 3.4 kb tricistronic mRNA and no monocistronic *vp39b* mRNA. Since Fig. 3 shows that the VP39B protein was expressed *in vivo*, a cap-independent mechanism must therefore have been used to translate the VP39B protein from the tricistronic mRNA. After eliminating the possibility of ribosomal reinitiation (Figs. 4 and 5), taking all these data together, we conclude that the expression of VP39B protein is regulated *in vivo* by an internal ribosome entry site (IRES). The RRL and Sf9 experiments further showed that the IRES element was located in the IRES$_{123–919}$ fragment (Figs. 5 and 6). There are several observations to be made on these experiments. First, we note that IRES activity was low both in the Sf9 cells (64.3 ± 12.9%) and in the RRL compared to the cap-dependent expression of RL (Figs. 5 and 6). This may be because these systems lack the specific IRES *trans*-acting factors (ITAFs). It is likely that Sf9 insect cells lack some of the ITAFs that are present in shrimp cells, while RRL has been shown to lack ITAFs that are necessary for IRES-dependent translation initiation (Byrd et al., 2005; Pudi et al., 2003). It is also possible that the fusion of the N-terminal region of *vp39b* to FL in the plasmids might have interfered with the translational efficiency of FL and/or affected its activity.

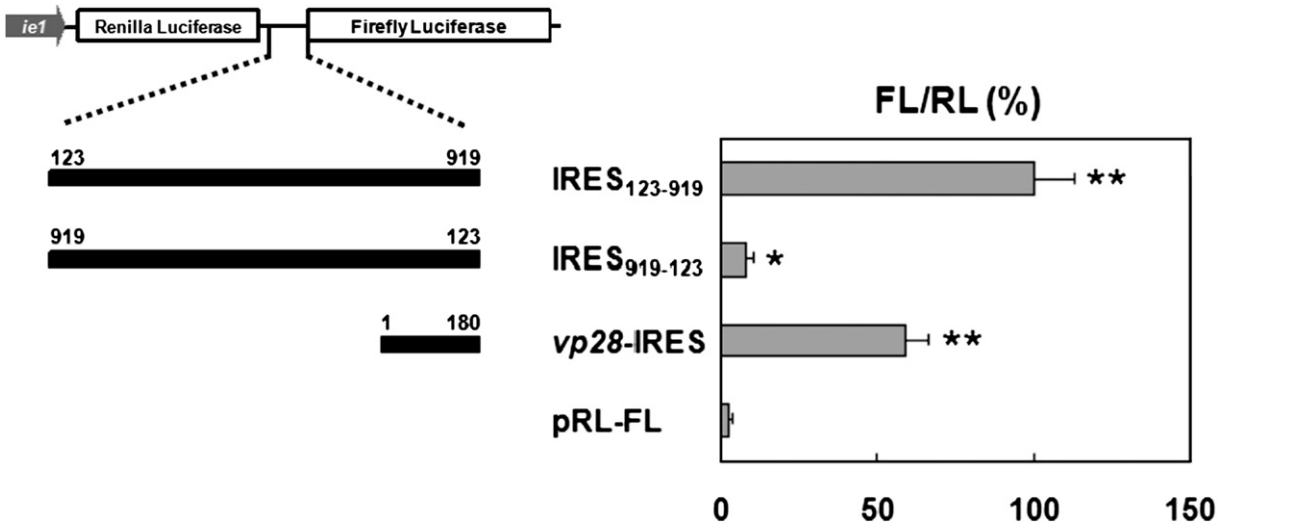

Fig. 6. The IRES element is active in Sf9 cells. The indicated IRES$_{123–919}$, IRES$_{919–123}$ and *vp28*-IRES fragments were cloned into a bicistronic pRL-FL plasmid with a WSSV *ie1*(−94/+52) promoter and transfected into Sf9 cells. Cells were harvested 48 h post-transfection, and the *Renilla* and firefly luciferase activities were measured. The ratio of firefly to *Renilla* luciferase was used as an indicator of IRES activity. Values were adjusted relative to *ie1*/IRES$_{123–919}$, which was set to 100%. Three independent transfection assays were performed, and the mean ± SD was calculated. (*P<0.05, **P<0.001 by one-way analysis of variance [ANOVA], relative to pRL-FL).

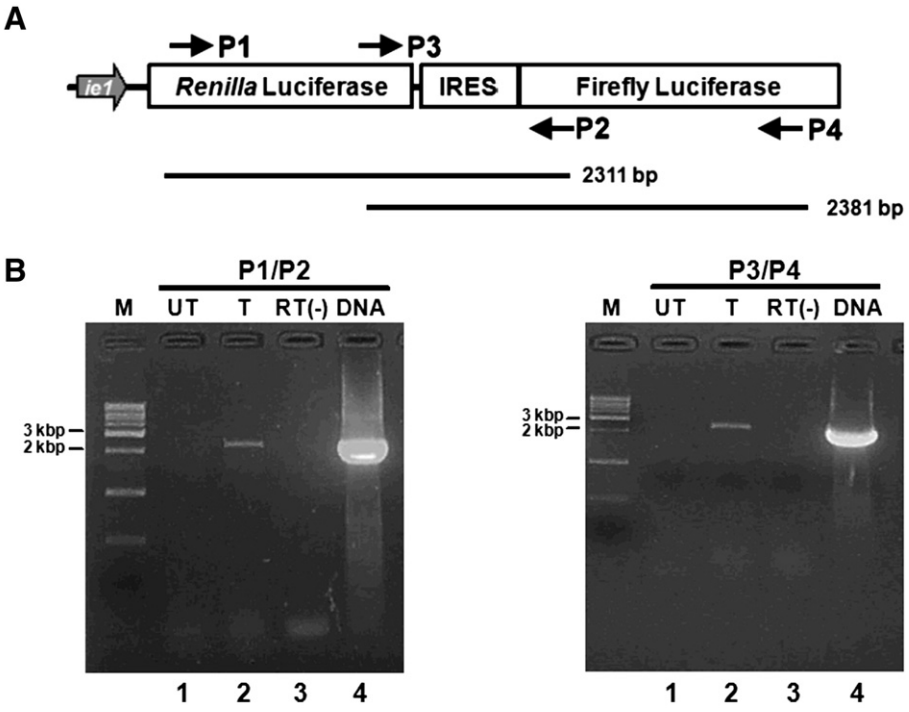

Fig. 7. The *ie1*/IRES$_{123–919}$ transcript has no internal splice sites. (A) Schematic diagram of the *ie1*/pRL-FL-based dicistronic construct and the two primer sets used for reverse transcription (RT)-PCR. The primers P1/P2 and P3/P4 represent pRL-FL-N219-F/pRL-FL-C1732-R and pRL-FL-N1071-F/pRL-FL-C2654-R, respectively (see Table 1). (B) RT-PCR results for total RNA extracted from Sf9 cells transfected (T) or untransfected (UT) with the *ie1*/IRES$_{123–919}$ bicistronic plasmid. In the negative RT(−) controls, RTase was omitted to verify that the RT-PCR products were specifically amplified from RNA and not from any contaminating plasmid DNA. The DNA lanes denote the PCR products from the *ie1*/IRES$_{123–919}$ plasmid and were used as a positive size control. Lane M shows 1 kb DNA ladder I markers (LAMDA Biotech Inc.).

Secondly, we observed that when the stem–loop plasmids were used to rule out the possibility of translational reinitiation, the reduction of the upstream RL translation enhanced downstream translation of the FL (cf Figs. 5C and D). To account for this, we hypothesize that in the absence of any competition with a cap-dependent mechanism, more free ribosomes would be available to load onto the IRES element to promote translational efficiency. Lastly, we note that translation of the positive control transcript (*vp28*-IRES) was much higher in the Sf9 cells than when it was translated from the stem–loop T7/SL-*vp28*-IRES plasmid in the RRL system (cf Figs. 5D and 6). Although we do not know the reason for this, similar discrepancies have been reported for other IRES elements under different experimental conditions (Collier et al., 1998; Creancier et al., 2000; Hennecke et al., 2001; Kamoshita et al., 1997; Woolaway et al., 2001).

Although most IRES elements are located within the 5′ UTR or intergenic region of the mRNA, the IRES element that we identified here is located in the *vp31*/*vp39* coding region. This is unusual, and to date, only a few IRESs have been found within the coding sequences of DNA or RNA viruses. These include an IRES located in the vCyclin ORF of KSHV (Bieleski and Talbot, 2001; Low et al., 2001), an IRES located in the VP2 ORF of SV40 (Yu and Alwine, 2006), and an IRES in the gag coding region of human immunodeficiency virus type 1 (Buck et al., 2001). Collectively, these IRES elements might represent a novel type of IRES, but their regulating mechanism remains unknown. Further study will be needed to discover how these elements can function as IRESs while still being part of the translatable coding region.

Our Northern blot analysis of the *vp60b*/*wssv478*/*wssv479*/*vp28* gene cluster detected at least three transcripts (~3.4 kb, 1.3 kb, 1.0 kb) using the *vp28*-specific probe (Fig. 1B). Analysis of the 3.4 kb polycistronic RNA by 5′/3′ RACE revealed that *vp60b* and *vp28* were both present and that they shared the same TIS and poly(A) tail. Marks et al. (2003) found that the TIS of *vp28* was located only 33 nt upstream of the transcription start codon (TAA**C**), which almost matches our unpublished TIS data (TAAC**C**) for the 1.0 kb monocistronic *vp28* mRNA. By contrast, Zhang et al. (2002) found that the TIS of *vp28* from a cDNA clone was located 482 nt upstream of the transcription start codon. This is consistent with the 1.3 kb *wssv479*/*vp28* bicistronic mRNA detected in Fig. 1B. Using the same cDNA clone, Han and Zhang (2006) were subsequently the first to identify a 180 bp IRES element in the 5′ UTR of *vp28*, and infer that it was downstream of an in-frame minicistron of about 5 kDa. Taking all these data together with our Northern blot results, we conclude that there are at least three TISs for *vp28*, one in the 5′ UTR of the *vp60b*/*wssv478*/*wssv479*/*vp28* polycistronic mRNA, one in the 5′ UTR of the *wssv479*/*vp28* bicistronic mRNA, and one in the 5′ UTR of the monocistronic *vp28* mRNA.

Analysis of the WSSV genome reveals many structural and non-structural genes that occur in clusters. In addition to the four clusters studied here, i.e. *vp60b*(−)/*wssv478*(−)/*wssv479*(−)/*vp28*(+), *wssv130*(+)/*wssv133*(−)/*vp36a*(+), *vp36b*(+)/*vp51b*(+)/*vp38a*(+), and *vp31*(−)/*vp39b*(−)/*vp11*(+), these include *vp22*(−)/*vp39a*(−)/*wssv363*(−)/*vp51c*(+), *vp41a*(−)/*vp51a*(+)/*vp41b*(−)/*wssv299*(+), *wssv237*(−)/*wssv240*(+)/*wssv243*(+), *wssv285*(+)/*wssv287*(−)/*wssv288*(+), and *wssv038*(−)/*wssv035*(−)/*wssv033*(+), where the plus sign indicates a poly(A) signal near the stop codon of the gene. We have shown that the four gene clusters studied here all transcribe a polycistronic mRNA with a shared poly(A) tail (Fig. 1B), and we hypothesize that this is also probably true for most of the other gene clusters. This is especially likely for clusters such as *vp22*/*vp39a*/*wssv363*/*vp51c*, where the polyadenylation signal can only be identified within the ORF or the 3′ UTR of the last gene. Further, as shown by the present paper for *vp39b*, and by Han and Zhang (2006) for *vp28*, IRES elements are used to regulate the translation of these two polycistronic mRNAs, and it seems likely that an IRES mechanism is also being used to regulate translation of the polycistronic mRNAs transcribed from many of these other WSSV structural/non-structural gene clusters.

Although the significance of an IRES mechanism in WSSV gene expression is presently unknown, Gale et al. (2000) point out that a translational mechanism like IRES can be used to ensure that structural proteins can still be expressed even under unfavorable conditions, such

as when virus-induced host shutoff decreases cap-dependent translation efficiency. For example, some RNA viruses (e.g., Picornavirus) use an IRES element cap-independent translational mechanism to enable selective translation of viral mRNA during host shutoff (Belsham and Sonenberg, 1996; Gale et al., 2000). Other cap-independent mechanisms can also be used to achieve similar results. For example, Human papillomavirus transcripts, which are almost all bicistronic or polycistronic mRNAs, use translational control mechanisms such as leaky scanning or translational reinitiation to translate downstream ORFs (Zheng and Baker, 2006). In the case of WSSV, we hypothesize that IRES elements are being used to ensure the translation of important viral structural proteins (including *vp28* and *vp39b*), which in turn would allow the virion to be successfully assembled. This hypothesis will need to be further explored in future studies.

Materials and methods

Virus purification of intact WSSV virions and fractionation of virion proteins

The virus used in this study, WSSV Taiwan isolate WSSV-TW (Lo et al., 1999), was originally isolated from a batch of WSSV-infected *Penaeus monodon* shrimp collected in Taiwan in 1994 (Wang et al., 1995). For proliferation and purification of intact WSSV virions from crayfish and for the fractionation of virion proteins into envelope and capsid proteins, we followed the methods described by Xie et al. (2006).

WSSV infection of P. monodon

Adult *P. monodon* (30 to 40 g) were collected from a culture pond in Tung Kang. The shrimps used for the challenge test were checked with a commercial WSSV diagnostic kit (IQ2000™, IntelliGene) and confirmed to be WSSV-free. Experimental shrimps were infected with WSSV by injection between the fourth and fifth abdominal segments using a method described previously (Tsai et al., 1999). Immediately before injection and at 60 h post injection (hpi), the pleopods, lymphoid organs, and gills of two randomly selected shrimps were excised, immediately frozen in liquid nitrogen and then stored in liquid nitrogen until used.

Transcriptional analysis of WSSV genes by Northern blot

About 20 μg of total RNA isolated from the pleopods or gills of WSSV-infected *P. monodon* was subjected to electrophoresis in 1% formaldehyde gel. RNA was transferred onto positively charged nylon membranes (Roche Applied Science) with 20× SSC overnight, and detected by digoxigenin (DIG)-labeled RNA probes (DIG System Users Guide from Roche Applied Science). The *vp60b*, *vp28*, *vp36a* and *vp38a* fragments used for the DIG-labeled probes were amplified from WSSV genomic DNA by PCR with primer sets *vp60b*-F/*vp60b-R*, *vp28*-F/*vp28*-R, *vp36a*-F/*vp36a*-R and *vp38a*-F/*vp38a*-R respectively (Table 1). The amplified fragments (10 to 25 ng) were ligated with T7 adaptor (5′-CATTAATG-CAGCTGGCTTATCGAAATTAATACGACTCACTATAGGGAGA-3′) using T4

Table 1
primers used in this study

Primer name	Sequence	Usage
vp31-EcoRI-F1	5′-GAATTCGATGTCTAATGGCGCAAC-3′	Antibody preparation
vp31-NotI-R1	5′-AGGCGGCCGCTTACTCCTCCTTAAAAGCAG-3′	Antibody preparation/riboprobe for vp31
vp39b-BamHI-F1	5′GAGGATCCAATGTCGTCTAACGGAGATG-3′	Antibody preparation
vp39b-EcoRI-R1	5′-ATGAATTCCTAAAAAACAAACAGATTGAAATC-3′	Antibody preparation/plasmid construction for TNT
vp11-N148-BamHI-F1	5′-GTGGATCCATATAAATTAGACTCTAAATACAC-3′	Antibody preparation
vp11-C538-HindIII-R1	5′-TTCAAGCTTAATTGGTAGATTTTTGTGCAAC-3′	Antibody preparation
vp31-5′-RACE-sp1	5′-ATACCAATGTACAAGATTTTGCGTTAG-3′	5′RACE for vp31
vp39b-5′-RACE-sp1	5′-GGATTGAAAGCGTCTTCGTAAAGATG-3′	5′RACE for *vp39b*
vp11-5′-RACE-sp1	5′-GCTCTCTCGTTTGACGTTGAAGCGCTG-3′	5′RACE for *vp11*
vp31-5′-RACE-sp2	5′-AGGCGAGATCTCACATCCAGTTCTGCATCC-3′	5′RACE for vp31
vp39b-5′-RACE-sp2	5′-CCGAATAGGCAATTGCACCTAAGCG-3′	5′RACE for vp39b
vp11-5′-RACE-sp2	5′-GTCGTCAGTTTTTTCATCATCGTCAGTG-3′	5′RACE for vp11
wssv397-R1	5′-CTGGTCAAGTAGGGCGGTGT-3′	3′RACE for vp31
vp39b-R2	5′-GGATCATGGAACCCAGGGAA-3′	3′RACE for vp39b/riboprobe for vp39b
vp11-3′RACE	5′-GCTCTGCAAGCACAGCTAAGG-3′	3′RACE for vp11
vp31-BamHI-F2	5′-GGGGATCCATGTCTAATGGCGCAACTATAAG-3′	Riboprobe for vp31
vp39b-F2	5′-CGAATCCTCGGATGGGTTGA-3′	Riboprobe for vp39b
vp11-F2	5′-AGCGTATACCCGTACACGGT-3′	Riboprobe for vp11
vp11-R2	5′-AGACCCAGACGCAGAAATGG-3′	Riboprobe for vp11
vp36a-F	5′-ATGGATCCAATGGCATTACAGGAAAAGG-3′	DIG-labeled probe for vp36a
vp36a-R	5′-GGAAGCTTTCAAACTACTACTATACATATT-3′	DIG-labeled probe for vp36a
vp60b-F	5′-GGGGATCCGATTGATAGGAGCGGAATTG-3′	DIG-labeled probe for vp60b
vp60b-R	5′-TTGAATTCTTACGTCGATAGCCAAAAGCTTTG-3′	DIG-labeled probe for vp60b
vp28-F	5′-CCCATATGGATCTTTCTTTCACTCTTTC-3′	DIG-labeled probe for *vp28*
vp28-R	5′-CCCTCGAGTTACTCGGTCTCAGTGCCAGAGT-3′	DIG-labeled probe for vp28
vp38a-F	5′-AAGGATCCCATGTCTTCTTCGTCTTCTG-3′	DIG-labeled probe for *vp38a*
vp38a-R	5′-AAGAATTCTTATGAACATGTTACAATTATTCG-3′	DIG-labeled probe for vp38a
vp31-BamHI-F3	5′-AGGGATCCCATGTCTAATGGCGCAACTATAAG-3′	Plasmid construction for TNT
vp31-MU491(T→A)	5′-TAGTTTCGTTCCATAAATGATGAGGATG-3′	Plasmid construction for TNT
vp31-REV489	5′-TTTTGCCGTTATTTTAAAATCTCCCAAGG-3′	Plasmid construction for TNT
vp31-D4FS-BamHI-F4	5′-GGGGATCCAATGCTAATGGCGCAACTAT-3′	Plasmid construction for TNT
ie1 promoter-SacI-F	5′-AGGAGCTCCCTTGTTACTCATTTATTCCTA-3′	Plasmid construction for dual luciferas assay
ie1 promoter-NheI-R	5′-CCGCTAGCCTTGAGTGGAGAGAGAGA-3′	Plasmid construction for dual luciferas assay
vp31-IRF1-N123-SmaI	5′-CACCCGGGCGAATTGTTGAAGAACACTG-3′	Plasmid construction for dual luciferas assay
vp39b-IRR1-C919-NcoI	5′-AACCATGGCTAAGCGATACTTTAATTG-3′	Plasmid construction for dual luciferas assay
vp39b-IRF1-C919-SmaI-F	5′-AACCCGGGCTAAGCGATACTTTAATTGG-3′	Plasmid construction for dual luciferas assay
vp31-IRR1-N123-NcoI-R	5′-CACCATGGCGAATTGTTGAAGAACACTG-3′	Plasmid construction for dual luciferas assay
*vp28*IRES-SmaI-F	5′-TGCCCGGGTAGACCCTGGCTTACTGTA-3′	Plasmid construction for dual luciferas assay
*vp28*IRES-NcoI-R	5′-TCCCATGGGACGAGTTTTTTTCTTTATC-3′	Plasmid construction for dual luciferas assay
pRL-FL-N219-F	5′-GTCCGCAGTGGTGGGCCAGATG-3′	RT-PCR assay
pRL-FL-C1732-R	5′-CGAAGGACTCTGGCACAAAATCGT-3′	RT-PCR assay
pRL-FL-N1071-F	5′-CGTTCGTTGAGCGAGTTCTC-3′	RT-PCR assay
pRL-FL-C2654-R	5′-GTCATCGTCTTTCCGTGCTC-3′	RT-PCR assay

ligase (Promega). The ligation products (1 μl) were subjected to PCR amplification by gene-specific forward primer (*vp60b*-F for *vp60b*, *vp28*-F for *vp28*, *vp36a*-F for *vp36a* and *vp38a*-F for *vp38a*) and T7 adaptor primer 1 (5′-CATTAATGCAGCTGGCTTATCGAAAT-3′) to generate probes with the T7 promoter. DIG-labeled antisense RNA probes were then made by *in vitro* transcription at 37 °C for 2 h with 2 μl of 5× DIG-RNA labeling mix (Roche Applied Science), 40 U of T7 RNA polymerase (Promega), 4 μl of 5× transcription buffer and 100–200 ng of the corresponding gene-specific probe to a final volume of 20 μl. The resulting DIG-labeled RNA probes were treated with 2 μl of DNase I (RNase-free; Invitrogen) at RT for 15 min. This was followed by DNase I inactivation by the addition of 2 μl 25 mM EDTA and incubation at 65 °C for 10 min to stop the reaction. The DIG-labeled RNA probes were denatured by heating at 95 °C for 5 min and cooling quickly on ice for 1 min, and then mixed with preheated (68 °C) hybridization buffer (50% formamide [v/v] deionized, 5× SSC, 0.1% N-lauroylsarcosine [w/v], 0.02% SDS [w/v], 2% blocking solution [1/5 volume of 10× blocking solution]). Hybridization and detection were performed as described in the DIG System Users Guide from Roche Applied Science. After 16 h hybridization at 68 °C, the membranes were washed twice with 2× SSC/0.1% SDS at RT for 5 min, and then washed twice with 0.1× SSC/0.1% SDS at 68 °C for 15 min. The membranes were incubated with anti-digoxigenin-AP, Fab fragment (1:20,000 dilution) (Roche Applied Science), detected with CDP-Star, ready-to-use (Roche Applied Science), and exposed to X-ray film at RT for 30 min.

About 30 μg of total RNA isolated from the pleopods of WSSV-infected *P. monodon* was separated on a 1% formaldehyde gel, and transferred onto Hybond-N^+ nylon membranes (Amersham Pharmacia Biotech, USA) as described by Sambrook et al. (1989). The *vp31*, *vp39b*, and *vp11* fragments used for riboprobe preparation were amplified from WSSV genomic DNA by PCR with the primer sets *vp31*-BamHI-F2/*vp31*-NotI-R1, *vp39b*-F2/*vp39b*-R2, and *vp11*-F1/*vp11*-R1, respectively (Table 1). Radioactively labeled *vp31*-, *vp39b*-, and *vp11*-specific probes were then generated as described previously (Chen et al., 2002). The membranes were prehybridized at 65 °C for 1 h with prehybridization buffer (0.25 M sodium phosphate buffer [0.5 M Na_2HPO_4, 0.5 M NaH_2PO_4], 1 mM EDTA, 1% BSA, 7% SDS), and then hybridized with the *vp31*-, *vp39b*- and *vp11*-specific [α-^{32}P] rCTP-labeled riboprobes at 65 °C for 16 h. Membranes were washed for 5 min with wash buffer I (2× SSC and 0.5% SDS) at room temperature, 30 min with wash buffer II (2× SSC and 0.1% SDS) at 65 °C, and 30 min with wash buffer III (0.1× SSC and 0.1% SDS) at 65 °C, and then exposed to Kodak BioMax MR film with a intensifying screen for several days at −80 °C.

5′ and 3′ RACE

5′ and 3′ RACEs were conducted for all three genes to find their corresponding 5′ and 3′ ends. The frozen lymphoid organs from the WSSV-infected *P. monodon* at 60 hpi were homogenized with Trizol reagent (Invitrogen) to extract the total RNA, and 5′ RACE was performed using a commercial FirstChoice® RLM-RACE kit (Ambion, Inc., Austin, Tex.) according to the instruction manual. Briefly, DNase I-treated total RNA was reacted with calf intestine alkaline phosphatase, and then treated with tobacco acid pyrophosphatase to remove the 5′ cap structure, leaving a 5′-monophosphate. The full-length decapped RNA was then ligated to a 45 bp RNA adapter with T4 RNA ligase. Reverse transcription was performed by M-MLV reverse transcriptase with random decamers from the kit. The first round PCR was conducted with the 5′ RACE outer primer (supplied with the kit) and the first gene-specific primers: *vp31*-5′-RACE-sp1, *vp39b*-5′-RACE-sp1, and *vp11*-5′-RACE-sp1 for *vp31*, *vp39b*, and *vp11* respectively (Table 1). The second round PCR was performed with the 5′ RACE inner primer (supplied with the kit) and the second gene-specific primers: *vp31*-5′-RACE-sp2, *vp39b*-5′-RACE-sp2, and *vp11*-5′-RACE-sp2 (Table 1). For 3′ RACE, the first strand cDNA was synthesized using an oligo(dT)-anchor primer (Roche Molecular Biochemicals), and then amplified with a gene-specific forward primer (*wssv397*-R1 for *vp31*, *vp39b*-R2 for *vp39b*, *vp11*-3′RACE for *vp11*, Table 1) and an anchor primer. The PCR products of the 5′ and 3′ RACE were cloned into the vector pGEM-T (Promega) and sequenced.

Antibody preparation

The full length coding regions of *vp31* (nt 1–786) and *vp39b* (nt 1–852), and a partial coding region of *vp11* (nt 148–570) were amplified by the primer sets *vp31*-EcoRI-F1/*vp31*-NotI-R1, *vp39b*-BamHI-F1/*vp39b*-EcoRI-R1 and *vp11*-N148-BamHI-F1/*vp11*-C538-HindIII-R1, respectively (Table 1). The corresponding PCR products were digested by the appropriate restriction enzymes and then cloned into pET28b (+). The recombinant proteins were expressed in BL21 Codon Plus *Escherichia coli* cells (Stratagene) and purified using Ni-NTA beads as previously described (Leu et al., 2005). The purified proteins were eluted directly from the beads with sodium dodecyl sulfate (SDS) sample buffer, and then subjected to SDS polyacrylamide gel electrophoresis (SDS-PAGE) analysis. The protein bands were sliced from the gel, minced, and mixed with Freund's adjuvant for antibody production in rabbit.

Western blot analysis

The purified virions, envelope and nucleocapsid fractions were separated by SDS-PAGE, and then transferred onto a polyvinylidene difluoride (PVDF) membrane (MSI). After incubation in blocking buffer (5% skim milk, 50 mM Tris, 500 mM NaCl, pH 7.5, 0.5% Tween 20) at 4 °C overnight, the PVDF membranes were reacted with anti-VP31, anti-VP39B, anti-VP11 and anti-VP51C antibody (1:5000 dilution in blocking buffer) for 1 h at room temperature, and then washed twice with TBS-T (50 mM Tris, 500 mM NaCl, pH 7.5, 0.5% Tween 20). Membranes were incubated with a horseradish peroxidase-conjugated anti-rabbit immunoglobulin G antibody as the secondary antibody (1:5000 dilution in TBS-T) for 1 h, and then washed twice with TBS-T. A chemiluminescence system (Perkin Elmer, Inc.) was used for detection.

Plasmid construction

To produce the plasmid pcDNA3-HA-*vp31*/*vp39b*, the *vp31*/*vp39b* coding region (1641 nt) was amplified using Pfu DNA polymerase (MDBio, Inc.) with primers (*vp31*-BamHI-F3/*vp39b*-EcoRI-R1; Table 1) containing a BamHI restriction site and a blunt-end. The PCR product was then cloned to the vector pcDNA3 (Invitrogen) upstream of a hemagglutinin (HA)-tag using BamHI and EcoRV restriction sites. A truncation plasmid, pcDNA3-HA-*vp31*-T/*vp39b*, was also produced. In this plasmid the primer sets *vp31*-BamHI-F3/*vp31*-REV489 and *vp31*-MU491(T→A)/*vp39b*-EcoRI-R1 (Table 1) were used to mutate the second base "T" of codon 164 of *vp31* into an "A" so as to produce a stop codon. The third plasmid, pcDNA3-HA-*vp31*-F/*vp39b*, was a frame shift mutation, in which the primer set *vp31*-D4FS-BamHI-F4/*vp39b*-EcoRI-R1 (Table 1) was used to eliminate the fourth base "T" from the second codon in *vp31* to produce a 20-codon nonsense open reading frame.

The pRL-FL plasmid was constructed as described previously (Bieleski and Talbot, 2001), that is, the firefly luciferase from pGL3 plasmid (Promega) was inserted into pRL-null plasmid (Promega) to give the dual luciferase plasmid T7/pRL-FL. For transient DNA transfection in Sf9 cells, the WSSV *ie1* promoter (−94/+52) (Liu et al., 2007) was used to replace the T7 promoter by amplification (*ie1* promoter-SacI-F/*ie1* promoter-NheI-R; Table 1) and cloning the promoter into the SacI-NheI sites of T7/pRL-FL to produce the construct *ie1*/pRL-FL. The putative *vp31*/*vp39b* IRES fragment and its antisense sequence (as a negative control) were PCR amplified (primer

sets *vp31*-IRF1-N123-SmaI/*vp39b*-IRR1-C919-NcoI and *vp39b*-IRF1-C919-SmaI-F/*vp31*-IRR1-N123-NcoI-R, respectively; Table 1) and cloned into *ie1*/pRL-FL to generate *ie1*/IRES$_{123–919}$ and *ie1*/IRES$_{919–123}$. As a positive control, the IRES element (180 bp) of *vp28* was PCR amplified (primer set *vp28*IRES-SmaI-F/*vp28*IRES-NcoI-R) and inserted into *ie1*/pRL-FL to generate the plasmid *ie1*/*vp28*-IRES. The empty vector *ie1*/pRL-FL was also used as a negative control for IRES activity. For *in vitro* translation, we used the plasmids T7/IRES$_{123–919}$, T7/IRES$_{919–123}$, T7/*vp28*-IRES, and T7/pRL-FL. These were identical to *ie1*/IRES$_{123–919}$, *ie1*/IRES$_{919–123}$, *ie1*/*vp28*-IRES, and *ie1*/pRL-FL except that they used the original T7 promoter. To block ribosome scanning *in vitro*, a stable 28-bp stem–loop ($\Delta G = -62$ kcal/mol) made of a 60-nucleotide sequence (5′-GCTAGCGGTACGGCAGTGCCGTACGAC-GAATTCGTCGTACGGCACTGCCGTACCGCTAGC-3′; Bieleski and Talbot, 2001) was cloned at the NheI site immediately upstream from the *Renilla* luciferase start codon to produce the plasmids T7/SL-IRES$_{123–919}$, T7/SL-IRES$_{919–123}$, T7/SL-*vp28*-IRES and T7/SL-pRL-FL.

Coupled in vitro transcription-translation reactions

In vitro transcription and translation assays were carried out using the TNT® Quick Coupled Transcription/Translation Systems (Promega Inc.) according to the manufacturer's instructions. Briefly, 1 μg of plasmid DNA was added to 50 μl of translation mixture containing 1 μl [^{35}S] methionine (1000 Ci/mM, EASYTIDES™) and incubated for 90 min at 30 °C. The reaction products (10 μl) were then added to 10 μl of 2× SDS sample buffer for resolution by SDS-PAGE. After electrophoresis, the gel was dried, and exposed to X-ray film at room temperature for 16 h.

In vitro transcription

RNA transcripts were prepared using a RiboMAX™ Large Scale RNA Production System-T7 kit (Promega) as described by the technical manual. The various T7/pRL-FL based constructs were linearized with NotI, and T7 RNA polymerase (Promega) was used to transcribe uncapped transcripts from the linearized plasmid DNAs (1 μg) at 37 °C for 2 h. The DNA template was then removed by digestion using RNase-free DNase I (Invitrogen) as described above. RNA sizes were determined by separating the RNAs on 1% agarose-formaldehyde gel.

In vitro translation

In vitro translation of the uncapped transcripts was performed by Flexi Rabbit Reticulocyte Lysate (RRL; Promega) according to the manufacturer's instructions. RNA (1.5 μg) was added to 25 μl reaction mixtures containing 16.5 μl of RRL, 1 μl of [^{35}S] methionine, 0.5 μl of amino acid mixture minus methionine, 0.5 μl of RNasin® ribonuclease inhibitor (40 U/μl; Promega), 0.5 μl of 100 mM DTT, and 0.4 μl of 2.5 M potassium chloride (final potassium ion concentration was 40 mM) and incubated at 30 °C for 90 min. An aliquot of the reaction products (5 μl) was then added to 5 μl of 2× SDS sample buffer and analyzed by SDS-PAGE and autography as described above.

IRES activity assay for transfected Sf9 cells

For the IRES activity assays, Sf9 cells were seeded in 24-well trays (1×10^5 cells/well) and grown in Sf-900 II SFM serum-free medium (Invitrogen) overnight at 27 °C. Plasmid DNAs (0.5 μg of plasmid DNA per well) were transfected into Sf9 cells using the Cellfectin reagent (Invitrogen) according to the manufacturer's recommendations. Cells were harvested at 48 h after transfection and analyzed for dual luciferase activities using the Dual-Luciferase® Reporter Assay System (Promega). Briefly, transfected cells were washed twice with 1× PBS, lysed with 100 μl of passive lysis buffer, and then incubated for 15 min at RT on an orbital shaker with gentle shaking. Cell lysate (20 μl) were used to measure luciferase activities with a Labsystems benchtop luminometer. The ratio of firefly luciferase activity to *Renilla* luciferase activity was used as an index of IRES activity. Transfection assays were performed in triplicate with three independent experiments, each using a different batch of purified plasmid DNA. Data are presented as mean ± SD (standard derivation) from the three triplicate experiments.

Reverse transcription-PCR analysis

Total RNA (1 μg) isolated by Trizol reagent (Invitrogen) from untransfected and transfected Sf9 cells was pretreated with DNase I and then reverse transcribed by SuperScript II Reverse Transcriptase (Invitrogen). PCR was performed with the primer sets pRL-FL-N219-F/pRL-FL-C1732-R and pRL-FL-N1071-F/pRL-FL-C2654-R (Table 1) using the following profile: 94 °C for 3 min; 30 cycles at 94 °C for 1 min, 60 °C for 30 s, and 72 °C for 2 min; a final extension at 72 °C for 20 min. The PCR products were then cloned into the vector pGEM-T (Promega) and sequenced.

Acknowledgments

This investigation was supported financially by National Science Council grants (NSC95-2311-B-002-016-MY3-2, NSC95-2311-B-002-016-MY3-3). Our thanks go to Mr. Kuan-Fu Liu of Tung Kang Marine Laboratory, Taiwan Fisheries Research Institute for providing the cultured *P. monodon* used in our experiments. We are indebted to Paul Barlow for his helpful criticism.

References

Belsham, G.J., Sonenberg, N., 1996. RNA–protein interactions in regulation of picornavirus RNA translation. Microbiol. Rev. 60 (3), 499–511.
Bieleski, L., Talbot, S.J., 2001. Kaposi's sarcoma-associated herpesvirus vCyclin open reading frame contains an internal ribosome entry site. J. Virol. 75 (4), 1864–1869.
Buck, C.B., Shen, X., Egan, M.A., Pierson, T.C., Walker, C.M., Siliciano, R.F., 2001. The human immunodeficiency virus type 1 gag gene encodes an internal ribosome entry site. J. Virol. 75 (1), 181–191.
Byrd, M.P., Zamora, M., Lloyd, R.E., 2005. Translation of eukaryotic translation initiation factor 4GI (eIF4GI) proceeds from multiple mRNAs containing a novel cap-dependent internal ribosome entry site (IRES) that is active during poliovirus infection. J. Biol. Chem. 280 (19), 18610–18622.
Chen, L.L., Leu, J.H., Huang, C.J., Chou, C.M., Chen, S.M., Wang, C.H., Lo, C.F., Kou, G.H., 2002. Identification of a nucleocapsid protein (VP35) gene of shrimp white spot syndrome virus and characterization of the motif important for targeting VP35 to the nuclei of transfected insect cells. Virology 293 (1), 44–53.
Collier, A.J., Tang, S., Elliott, R.M., 1998. Translation efficiencies of the 5′ untranslated region from representatives of the six major genotypes of hepatitis C virus using a novel bicistronic reporter assay system. J. Gen. Virol. 79 (Pt 10), 2359–2366.
Creancier, L., Morello, D., Mercier, P., Prats, A.C., 2000. Fibroblast growth factor 2 internal ribosome entry site (IRES) activity ex vivo and in transgenic mice reveals a stringent tissue-specific regulation. J. Cell Biol. 150 (1), 275–281.
Gale Jr., M., Tan, S.L., Katze, M.G., 2000. Translational control of viral gene expression in eukaryotes. Microbiol. Mol. Biol. Rev. 64 (2), 239–280.
Griffiths, A., Coen, D.M., 2005. An unusual internal ribosome entry site in the herpes simplex virus thymidine kinase gene. Proc. Natl. Acad. Sci. U. S. A. 102 (27), 9667–9672.
Grundhoff, A., Ganem, D., 2001. Mechanisms governing expression of the v-FLIP gene of Kaposi's sarcoma-associated herpesvirus. J. Virol. 75 (4), 1857–1863.
Han, F., Zhang, X., 2006. Internal initiation of mRNA translation in insect cell mediated by an internal ribosome entry site (IRES) from shrimp white spot syndrome virus (WSSV). Biochem. Biophys. Res. Commun. 344 (3), 893–899.
Hennecke, M., Kwissa, M., Metzger, K., Oumard, A., Kroger, A., Schirmbeck, R., Reimann, J., Hauser, H., 2001. Composition and arrangement of genes define the strength of IRES-driven translation in bicistronic mRNAs. Nucleic Acids Res. 29 (16), 3327–3334.
Jang, S.K., Krausslich, H.G., Nicklin, M.J., Duke, G.M., Palmenberg, A.C., Wimmer, E., 1988. A segment of the 5′ nontranslated region of encephalomyocarditis virus RNA directs internal entry of ribosomes during *in vitro* translation. J. Virol. 62 (8), 2636–2643.
Kamoshita, N., Tsukiyama-Kohara, K., Kohara, M., Nomoto, A., 1997. Genetic analysis of internal ribosomal entry site on hepatitis C virus RNA: implication for involvement of the highly ordered structure and cell type-specific transacting factors. Virology 233 (1), 9–18.
Kozak, M., 1978. How do eucaryotic ribosomes select initiation regions in messenger RNA? Cell 15, 1109–1123.
Kozak, M., 1987. Effects of intercistronic length on the efficiency of reinitiation by eucaryotic ribosomes. Mol. Cell. Biol. 7 (10), 3438–3445.

Leu, J.H., Tsai, J.M., Wang, H.C., Wang, A.H., Wang, C.H., Kou, G.H., Lo, C.F., 2005. The unique stacked rings in the nucleocapsid of the white spot syndrome virus virion are formed by the major structural protein VP664, the largest viral structural protein ever found. J. Virol. 79 (1), 140–149.

Liu, W.J., Yu, H.T., Peng, S.E., Chang, Y.S., Pien, H.W., Lin, C.J., Huang, C.J., Tsai, M.F., Huang, C.J., Wang, C.H., Lin, J.Y., Lo, C.F., Kou, G.H., 2001. Cloning, characterization, and phylogenetic analysis of a shrimp white spot syndrome virus gene that encodes a protein kinase. Virology 289 (2), 362–377.

Liu, W.J., Chang, Y.S., Wang, A.H., Kou, G.H., Lo, C.F., 2007. White spot syndrome virus annexes a shrimp STAT to enhance expression of the immediate-early gene ie1. J. Virol. 81 (3), 1461–1471.

Lo, C.F., Hsu, H.C., Tsai, M.F., Ho, C.H., Peng, S.E., Kou, G.H., Lightner, D.V., 1999. Specific genomic DNA fragment analysis of different geographical clinical samples of shrimp white spot syndrome virus. Dis. Aquat. Org. 35, 175–185.

Low, W., Harries, M., Ye, H., Du, M.Q., Boshoff, C., Collins, M., 2001. Internal ribosome entry site regulates translation of Kaposi's sarcoma-associated herpesvirus FLICE inhibitory protein. J. Virol. 75 (6), 2938–2945.

Marks, H., Mennens, M., Vlak, J.M., van Hulten, M.C., 2003. Transcriptional analysis of the white spot syndrome virus major virion protein genes. J. Gen. Virol. 84 (Pt 6), 1517–1523.

Pelletier, J., Sonenberg, N., 1988. Internal initiation of translation of eukaryotic mRNA directed by a sequence derived from poliovirus RNA. Nature 334 (6180), 320–325.

Pestova, T.V., Borukhov, S.I., Hellen, C.U., 1998. Eukaryotic ribosomes require initiation factors 1 and 1A to locate initiation codons. Nature 394 (6696), 854–859.

Poyry, T.A., Kaminski, A., Connell, E.J., Fraser, C.S., Jackson, R.J., 2007. The mechanism of an exceptional case of reinitiation after translation of a long ORF reveals why such events do not generally occur in mammalian mRNA translation. Genes Dev. 21 (23), 3149–3162.

Pudi, R., Abhiman, S., Srinivasan, N., Das, S., 2003. Hepatitis C virus internal ribosome entry site-mediated translation is stimulated by specific interaction of independent regions of human La autoantigen. J. Biol. Chem. 278 (14), 12231–12240.

Sambrook, J., Fritsch, E.F., Maniatis, T., 1989. Molecular Cloning: a Laboratory Manual, 2nd edn. Cold Spring Harbor Laboratory Press, Cold Spring Harbor, NY.

Tsai, M.F., Kou, G.H., Liu, H.C., Liu, K.F., Chang, C.F., Peng, S.E., Hsu, H.C., Wang, C.H., Lo, C.F., 1999. Long-term presence of white spot syndrome virus (WSSV) in a cultivated shrimp population without disease outbreaks. Dis. Aquat. Org. 38 (2), 107–114.

Tsai, M.F., Lo, C.F., van Hulten, M.C., Tzeng, H.F., Chou, C.M., Huang, C.J., Wang, C.H., Lin, J.Y., Vlak, J.M., Kou, G.H., 2000. Transcriptional analysis of the ribonucleotide reductase genes of shrimp white spot syndrome virus. Virology 277 (1), 92–99.

Tsai, J.M., Wang, H.C., Leu, J.H., Hsiao, H.H., Wang, A.H., Kou, G.H., Lo, C.F., 2004. Genomic and proteomic analysis of thirty-nine structural proteins of shrimp white spot syndrome virus. J. Virol. 78 (20), 11360–11370.

Tsukiyama-Kohara, K., Iizuka, N., Kohara, M., Nomoto, A., 1992. Internal ribosome entry site within hepatitis C virus RNA. J. Virol. 66 (3), 1476–1483.

van Hulten, M.C., Witteveldt, J., Peters, S., Kloosterboer, N., Tarchini, R., Fiers, M., Sandbrink, H., Lankhorst, R.K., Vlak, J.M., 2001. The white spot syndrome virus DNA genome sequence. Virology 286 (1), 7–22.

Wang, C.H., Lo, C.F., Leu, J.H., Chou, C.M., Yeh, P.Y., Chou, H.Y., E., T.M., Chang, C.F., Su, M.S., Kou, G.H., 1995. Purification and genomic analysis of baculovirus associated with white spot syndrome (WSBV) of *Penaeus monodon*. Dis. Aquat. Org. 23, 239–242.

Woolaway, K.E., Lazaridis, K., Belsham, G.J., Carter, M.J., Roberts, L.O., 2001. The 5′ untranslated region of *Rhopalosiphum padi* virus contains an internal ribosome entry site which functions efficiently in mammalian, plant, and insect translation systems. J. Virol. 75 (21), 10244–10249.

Xie, X., Xu, L., Yang, F., 2006. Proteomic analysis of the major envelope and nucleocapsid proteins of white spot syndrome virus (WSSV). J. Virol. 80 (21), 10615–10623.

Yang, F., He, J., Lin, X., Li, Q., Pan, D., Zhang, X., Xu, X., 2001. Complete genome sequence of the shrimp white spot bacilliform virus. J. Virol. 75 (23), 11811–11820.

Yu, Y., Alwine, J.C., 2006. 19S late mRNAs of simian virus 40 have an internal ribosome entry site upstream of the virion structural protein 3 coding sequence. J. Virol. 80 (13), 6553–6558.

Zhang, X., Huang, C., Xu, X., Hew, C.L., 2002. Identification and localization of a prawn white spot syndrome virus gene that encodes an envelope protein. J. Gen. Virol. 83 (Pt 5), 1069–1074.

Zheng, Z.M., Baker, C.C., 2006. Papillomavirus genome structure, expression, and post-transcriptional regulation. Front. Biosci. 11, 2286–2302.